SEMARAK ILMU PUBLISHING

Journal of Advanced Research in Fluid Mechanics and Thermal Sciences

Journal homepage:
https://semarakilmu.com.my/journals/index.php/fluid_mechanics_thermal_sciences/index
ISSN: 2289-7879

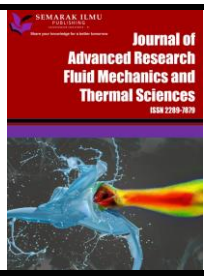

Effects of Hall Current, Diffusion Thermos and Activation Energy on MHD Radiative Casson Nanofluid Flow with Chemical Reaction and Thermal Radiation

Sridevi Dandu[1,*], Venkata Ramana Murthy Chitrapu[1], Udaya Bhaskara Varma Nadimpalli[2]

[1] Department of Engineering Mathematics, College of Engineering Koneru Lakshmaiah Education Foundation, Vaddeswaram-522502, A.P., India
[2] Department of Engineering Mathematics and Humanities, S. R. K. R. Engineering College, Bhimavaram-534204, West Godavari Dist, A.P., India

ARTICLE INFO

Article history:
Received 25 November 2022
Received in revised form 12 February 2023
Accepted 18 February 2023
Available online 12 March 2023

Keywords:
Hall current; thermal radiation; non-Newtonian fluid; MHD; heat generation; Brownian motion; thermophoresis

ABSTRACT

In this work, we studied the impact of Hall current, diffusion thermo, and activation energy on an electrically conducting Casson nanofluid flow past a continuously stretching surface with thermal radiation, and heat generation/absorption has been explored. Transverse magnetic field with the assumption of small Reynolds number is implemented vertically. Appropriate similarity transformations are utilized to transform the governing partial differential equations into the non-linear ordinary differential equations. Numerical solutions for the dimensionless velocity, temperature and nanoparticle concentration are computed with the help of the shooting method. Through the use of graphs, the discussion will focus on the effects that the Hall current, the thermal radiation, the heat source/sink, the Brownian motion, the thermophoresis parameter, and the magnetization have on velocity, concentration, and temperature. To get an insight into the internal behavior of the emerging parameters, a numerical calculation of the local Nusselt number, the Sherwood number, and the skin friction coefficient along the x-and z axes is performed. It has been shown that the resultant flow velocity enhances with increasing hall parameter, whereas it has reduced in temperature and concentration field. The temperature diminishes with improving diffusion thermo parameters, and the opposite behavior has been observed in the case of thermal radiation.

1. Introduction

The researcher has developed an interest in non-Newtonian fluids due to the extraordinary properties that these fluids exhibit in the technical and industrial sciences fields. Some common examples of non-Newtonian liquids are synthetic lubricants, drilling muds, oils, paints, sugar solutions, clay coatings, and biological fluids like blood. Other examples of non-Newtonian fluids include certain stains. Due to the complexity of the mathematical formulation of the flow issue, the basic Navier-Stokes equations cannot briefly specify the properties of the flow field of non-

* *Corresponding author.*
E-mail address: sridevidandu2005@gmail.com

https://doi.org/10.37934/arfmts.104.1.106123

Newtonian fluids. Abundant models for non-Newtonian fluids are defined as deliberate rheological qualities such as Eyring-Powell, Bulky, Seely, Oldroyd-B, Maxwell, Oldroyd-A, Carreau, Casson, Burger, Jeffrey, etc. Abundant models for non-Newtonian fluids are defined as deliberate rheological qualities such as Eyring-Powell, Bulky, Seely, Oldroyd-B, Maxwell, etc. Al-Khaled and Khan [1] have studied the Thermal aspects of Casson nano liquids, with gyrotactic microorganisms, temperature-dependent viscosity, and variable thermal conductivity. Ali *et al.,* [2] have investigated the finite element study of MHD impacts on the rotating flow of Casson nanofluid with the double diffusion Cattaneo-Christov heat flux model. Ghosh *et al.,* [3] have demonstrated bio-convective viscoelastic Casson nanofluid flow over a stretching sheet in an induced magnetic field with Cattaneo-Christov double diffusion. Wang *et al.,* [4] analyzed the numerical simulation of hybrid Casson nanofluid flow under magnetic dipoles and gyrotactic microorganisms. Prasad *et al.,* [5] have reviewed peristaltic activity in the blood flow of Casson nanoliquids with irreversibility aspects in the non-uniform vertical channel. Li *et al.,* [6] analyzed the effects of activation energy and chemical reaction on unsteady MHD dissipative Darcy–Forchheimer squeezed Casson fluid flow over the horizontal channel. Suresh Kumar *et al.,* [7] studied the numerical analysis of magnetohydrodynamic Casson nanofluid flow with activation energy, Hall current, and thermal radiation. Kodi *et al.,* [8] have discussed MHD Casson fluid flow past a vertical porous plate under the influence of thermal diffusion and chemical reaction. Kodi and Mopuri [9] expressed an unsteady MHD oscillatory Casson fluid flow past an inclined vertical porous plate in a chemical reaction with heat absorption and soret effects. Vaddemani *et al.,* [10] studied the characteristics of MHD Casson fluid flow past an inclined, vertical porous plate.

Nanofluid is a new class of fluid consisting of nanometer-sized particles suspended in a base fluid. Heat transfer fluids like water, ethylene glycol, and engine oil have low thermal conductivity. They are essential for the heat transfer coefficient between the medium and the surface. It has been proven through experiments that the thermal conductivity of nanofluid is appreciably higher than the base fluids. The term "nanofluid" was first coined by Choi and Eastman [11], who discovered that suspended nanoparticles in the base fluid could enhance the thermal conductivity of the base fluid efficiently. The nanoparticles are typically made of Al_2O_3, SiC, AlN, Cu, TiO, and graphite and have high thermal conductivity compared to conventional base fluids. Eastman *et al.,* [12] further explored that adding copper (10 nm) particles in ethylene glycol increases thermal conductivity by up to 40%. Later on, many researchers reported that adding 1–5% by volume of nanoparticles to ordinary heat transfer fluids can enhance thermal conductivity by more than 20%. Ahmad and Nadeem [13] studied the activation energy analysis and its impact on hybrid nanofluids in the presence of Hall and ion slip currents. Ahmad *et al.,* [14] have analyzed Maxwell nanofluids unsteady three-dimensional bioconvective flow over an exponentially stretching sheet with variable thermal conductivity and chemical reaction. Hou *et al.,* [15] have discussed the flow analysis of hybridized nanomaterial liquid flow in the presence of multiple slips and the Hall current effect over a slender stretching surface. Ahmad *et al.,* [16] studied the heat enhancement analysis of the hybridized micropolar nanofluid with Cattaneo–Christov and stratification effects. Ahmad and Nadeem [17] investigated thermal analysis in the buoyancy-driven flow of hybrid nanofluids subject to thermal radiation. Khan *et al.,* [18] studied the mathematical analysis of heat and mass transfer in a Maxwell fluid. Shah and Ullah [19] reviewed ferrofluid treatment by inserting an electric field inside a porous cavity and considering forced convection: entropy optimization and heat flux analysis of Maxwell nanofluid configured by an exponentially stretching surface with velocity slip. Shah *et al.,* [20] discussed the computational analysis of radiative engine oil-based Prandtl–Eyring hybrid nanofluid flow with variable heat transfer using the Cattaneo–Christov heat flux model. Tang *et al.,* [21] discussed the computational study and characteristics of magnetized gold-blood Oldroyd-B nanofluid flow and heat transfer in stenosed narrow arteries. Asghar *et al.,* [22] analyzed a magnetized mixed convection hybrid nanofluid with

heat generation, absorption, and velocity slip effects. Recently, Imtiaz Khan *et al.,* [23] have possessed the design of backpropagated intelligent networks for nonlinear second-order Lane–Emden pantograph delay differential systems. A recent researcher, AlDosari *et al.,* [24], explored drug release using nanoparticles in cancer cells on 2-D materials to target drug delivery: A numerical simulation via the molecular dynamics method, Engineering Analysis with Boundary Elements. Aljaloud *et al.,* [25] reviewed the bioconvection flow of Cross nanofluid due to the cylinder with activation energy and second-order slip features.

On the other hand, the combined effects of heat transfer, mass transfer, and chemical reaction play a significant part in the chemical and hydrometallurgical industries. The chemical reaction can be of any order; nevertheless, the chemical reaction of the first order is the simplest one because, in this kind of reaction, the reaction rate and the concentration of the species are proportional to one another. Smog production is an example of a chemical reaction that occurs in the first order. As a result of stretching a sheet, a chemical reaction between a foreign material and a working fluid often occurs in several processes used in chemical engineering. The quality of the final product significantly impacts the sorts of chemical reactions that may arise when diffusive species interact with the surrounding fluid. These reactions can either result in the absorption or generation of the species in question. Recently, Raghunath [26] has studied Heat and Mass Transfer of an Unsteady Magnetohydrodynamic Nanofluid Flow Past a Vertical Porous Plate in the Presence of Chemical Reaction, Radiation, and Soret Effects. Bafakeeh *et al.,* [27] have reviewed the Hall current and Soret effects on the unsteady MHD rotating flow of second-grade fluid through porous media under the influence of thermal radiation and chemical reaction. Raghunath and Mohanaramana [28] have analyzed Hall, Soret, and rotational effects on the unsteady MHD rotating flow of a second-grade fluid through a porous medium in the presence of chemical reaction and an aligned magnetic field. Tlili and Alharbi [29] have reviewed an investigation into the effect of changing the air quality and stream size on the Trombe wall for two different arrangements of rectangular blocks of phase change material in this wall. Dero *et al.,* [30] have expressed the contribution of the suction phenomenon and thermal slip effects for radiated hybrid nanoparticles (Al_2O_3-Cu/H_2O) with a stability framework. Banawas *et al.,* [31] have discussed reinforced calcium phosphate types of cement with zinc by changes in initial properties: A molecular dynamics simulation. Aljaloud *et al.,* [32] have proposed an investigation of phase change and heat transfer in water/copper oxide nanofluid enclosed in a cylindrical tank with a porous medium.

Hall current is most noticeable on the absolute magnitude and orientation of the current density and, as a result, on the magnetic force term. The convective flow issue with the magnetic field is crucial under the influence of Hall currents because of the technical usage in MHD accelerators, nanotechnological processing, nuclear energy systems using liquid metals, blood flow regulation, and heating components. The analysis of magnetohydrodynamic flows with Hall current is optimum for studying Hall accelerators and flight Magnetohydrodynamics when the magnetic field is of high intensity, and the gas density is relatively low. Peristaltic flows have many different uses under the influence of an applied magnetic field. Some examples of these applications include the magnetohydrodynamic property of blood, the process of dialysis, oxygenation, and hypothermia. Deepthi *et al.,* [33] have studied the Recent Development of Heat and Mass Transport in the Presence of Hall, Ion Slip, and Thermo Diffusion in Radiative Second Grade Material: Application of Micromachines. Ganjikunta *et al.,* [34] have analyzed an unsteady MHD flow of a second-grade fluid passing through a porous medium in the presence of radiation absorption exhibits Hall and ion slip effects. Kodi *et al.,* [35] studied Hall and ion slip radiative flow of chemically reactive second grade through porous saturated space via a perturbation approach. Rajakarunakaran *et al.,* [36] have analyzed, Prediction of strength and analysis in self-compacting concrete using machine learning

based regression techniques. Bai *et al.,* [37] have discussed Numerical analysis and two-phase modeling of water Graphene Oxide nanofluid flow in the riser condensing tubes of the solar collector heat exchanger. Okonkwo *et al.,* [38] have possessed Optimal sizing of photovoltaic systems based green hydrogen refueling stations case study Oman.

The heat carried away from the surface by thermal radiation is a significant contributor. Helicopters, space vehicles, trustworthy equipment design, satellites, atomic furnaces, missiles, space technology, and processes connected to high temperatures are examples of industrial businesses that might benefit from its implementation. Reddy *et al.,* [39]: Effect of Thermal Radiation on MHD Boundary Layer Flow of Nanofluid and Heat Transfer over a Non-Linearly Stretching Sheet with Transpiration. Kothandapani and Prakash [40] have discussed the effects of thermal radiation parameters and magnetic fields on the peristaltic motion of Williamson nanofluids in a tapered, asymmetric channel. Sulochana *et al.,* [41] have analyzed the thermal radiation effect on MHD nanofluid flow over a stretching sheet. Kho *et al.,* [42] have discussed thermal radiation effects on MHD with flow heat and mass transfer in Casson nanofluid over a stretching sheet. Raza [43] has studied thermal radiation and slip effects on Casson fluid's magnetohydrodynamic (MHD) stagnation point flow over a convective stretching sheet.

The study that Suresh Kumar *et al.,* [7] did was the foundation for the current investigation, which is an extension of that work. In this research, we investigated the effects of Hall current, diffusion thermo, and activation energy on an electrically conducting Casson nanofluid fluid flow past in a vertical direction when a chemical reaction and thermal radiation were present. The governing partial nonlinear differential equations of flow, heat, and mass transfer are transformed into ordinary differential equations via a similarity transformation. This allows for a more straightforward analysis. After that, the issues are solved using numerical methods. The consequences of several non-dimensional regulating parameters on velocity, temperature, and concentration profiles are discussed, and the results are shown graphically. When specific conditions are satisfied, the present study's findings show an exceptionally high degree of unity with the findings of previous investigations.

2. Formulation of the Problem

Here, steady heat and mass transfer of an incompressible hydromagnetic nanofluid flow along a vertical stretching sheet coinciding with the plane y = 0, has been considered in the presence of the Hall current effects. By keeping the origin fixed, two opposite and equal forces are assumed to employ along the x-axis so that the sheet stretches linearly in both positive and negative direction (see Figure 1).

i. With the assumption that the Newtonian nanofluid be electrically conducting and heat generating/absorbing, a strong magnetic field has been imposed normal to the direction of flow.
ii. Moreover, no electric field has been assumed to apply and the frequency of atom-electron collision has also been considered high for the generation of Hall current effect [44].
iii. Due to the strong magnetic flux density B_0, the Hall current effect is taken into consideration, however the small magnetic Reynolds number is employed and the induced magnetic field is ignored.
iv. Hall current effect is strong enough to give rise to a force in the z−direction and a cross flow is induced in the same direction which causes a three dimensional flow. It is further assumed that there are no variations in the flow, heat and mass transfer in the z-direction.

v. This assumption can be achieved by taking the sheet of infinite width. Non-conducting plate is considered so that the generalized Ohm's law in the flow field [45].
vi. Brownian motion and thermophoresis effects are considered using the Buongiorno model for the nanofluid [46]. Further, the effects of viscous dissipation and Joule heating are ignored.

The governing equations for Casson nanofluid along with continuity equation are followed by Suresh Kumar *et al.,* [7].

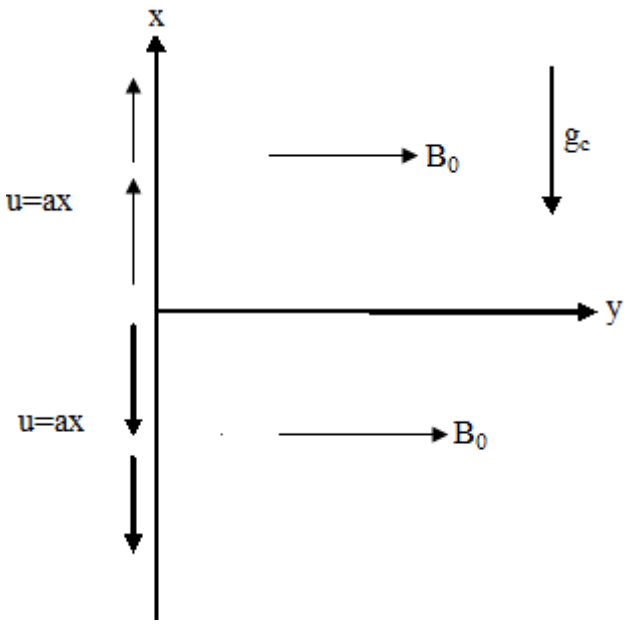

Fig. 1. Physical sketch and coordinate system

In light of the premises discussed earlier and the Boussinesq approach, the following is the arithmetical representation of the problem

$$\frac{\partial u}{\partial x}+\frac{\partial u}{\partial y}=0 \tag{1}$$

$$u\frac{\partial u}{\partial x}+v\frac{\partial u}{\partial y}=\nu\left(1+\frac{1}{\beta}\right)\frac{\partial^2 u}{\partial y^2}-\frac{\sigma B_0^2}{\rho\left(1+m^2\right)}\left(mw+u\right)+g_C\beta_T(T-T_\infty)+g_C\beta_C(C-C_\infty) \tag{2}$$

$$u\frac{\partial w}{\partial x}+v\frac{\partial w}{\partial y}=\nu\left(1+\frac{1}{\beta}\right)\frac{\partial^2 w}{\partial y^2}+\frac{\sigma B_0^2}{\rho\left(1+m^2\right)}\left(mu-w\right) \tag{3}$$

$$u\frac{\partial T}{\partial x}+v\frac{\partial T}{\partial y}=\frac{k}{\rho C_p}\frac{\partial^2 T}{\partial y^2}+\frac{Q_0}{\rho C_p}(T-T_\infty)+\tau\left(D_B\frac{\partial C}{\partial y}\frac{\partial T}{\partial y}+\frac{D_T}{T_\infty}\left(\frac{\partial T}{\partial y}\right)^2\right)-\frac{1}{\rho C_p}\frac{\partial q_r}{\partial y}+\frac{D_m k_T}{c_s c_p}\frac{\partial^2 C}{\partial y^2} \tag{4}$$

$$u\frac{\partial C}{\partial x}+v\frac{\partial C}{\partial y}=D_B\frac{\partial^2 C}{\partial y^2}+\frac{D_T}{T_\infty}\frac{\partial^2 T}{\partial y^2}-k_r^2\left(C-C_\infty\right)\left(\frac{T}{T_\infty}\right)^m\exp\left(\frac{-E_a}{K^*T}\right) \tag{5}$$

The associated boundary conditions for the PDEs that are in charge are as follows

$$\begin{aligned} &u=ax,\quad v=0,\quad w=0,\quad T=T_w,\quad C=C_w && \text{at } y=0\\ &u\to 0,\quad v\to 0,\quad w\to 0,\quad T\to T_\infty\quad C\to C_\infty && \text{as } y\to\infty \end{aligned} \tag{6}$$

The similarity conversion that was used so that the PDEs may be translated into dimensionless ODEs

$$\eta=\sqrt{\frac{a}{\nu}}y,\ \psi(x,y)=\sqrt{a\nu}\,x\,f(\eta),\ w=axg(\eta),\ \phi(\eta)=\frac{C-C_\infty}{C_w-C_\infty},\ \theta(\eta)=\frac{T-T_\infty}{T_w-T_\infty} \tag{7}$$

Because an optically thick fluid also engages in self-absorption in contrast to emission, the Rosseland approximation may be used for the radiative heat flux vector qr. We can use the Rosseland approximation because the absorption coefficient is often dependent on the wavelength and is substantial. As a result, the value serves as the description of qr.

$$q_r=\frac{-4\sigma_1}{3k^*}\frac{\partial^2 T^4}{\partial y} \tag{8}$$

The Rosseland mean absorption coefficient is expressed by the symbol k* in this expression, while the Stefan–Boltzmann characteristic is represented by the symbol σ_1.

Because we are functioning under the premise that the temperature fluctuations within the flow are not particularly important, we can define T^4 as a linear function. This gives us the ability to predict T^4 with high accuracy. We ignore higher-order variables as we proceed with the process of extending T^4 about the temperature of the free stream T using Taylor's series. A rough estimate may be found in the preceding, which can be obtained from this: The Rosseland mean absorption coefficient is expressed by the symbol k* in this expression.

$$T^4\approx 4T_\infty^3-3T_\infty^4 \tag{9}$$

Combining Eq. (8) and Eq. (9), one may arrive at an equation for energy, as shown in the succeeding.

$$\begin{aligned} u\frac{\partial T}{\partial x}+v\frac{\partial T}{\partial y}=\frac{k}{\rho C_p}\frac{\partial^2 T}{\partial y^2}+\frac{Q_0}{\rho C_p}(T-T_\infty)+\tau\left(D_B\frac{\partial C}{\partial y}\frac{\partial T}{\partial y}+\frac{D_T}{T_\infty}\left(\frac{\partial T}{\partial y}\right)^2\right)+\\ \frac{16\sigma_1 T_\infty^3}{3\rho C_p k^*}\frac{\partial^2 T}{\partial y^2}+\frac{D_m k_T}{c_s c_p}\frac{\partial^2 C}{\partial y^2} \end{aligned} \tag{10}$$

Substitute Eq. (7) into Eq. (2), Eq. (3), Eq. (5) and Eq. (10) generate to acquire the succeeding non-dimensional equations.

$$\left(1+\frac{1}{\beta}\right)f'''+ ff''- f'^2+Gr_x\theta+Gr_c\phi-\frac{M}{1+m^2}\left(f'+mg\right)=0 \tag{11}$$

$$\left(1+\frac{1}{\beta}\right)g''+ fg'- f'g+\frac{M}{1+m^2}\left(mf'-g\right)=0 \tag{12}$$

$$\theta''\left(1+R\,\mathrm{Pr}\right)+\mathrm{Pr}\ f\theta'+\mathrm{Pr}\,N_b\left(\theta'\phi'+\frac{N_t}{N_b}\theta'^2\right)+\mathrm{Pr}\,Q\,\theta+\mathrm{Pr}\,D_u\,\phi'=0 \tag{13}$$

$$\phi''+\mathrm{Pr}\ L_e\ f\ \phi'+\frac{N_t}{N_b}\theta''-K_E\left(1+\theta\right)^m\varphi\exp\left(\frac{-E}{1+\theta}\right)=0 \tag{14}$$

The dimensionless correlated boundary conditions (BCs) are as shadows

$$\begin{aligned} &f(0)=0,\quad f'(0)=1,\quad g(0)=0,\quad \theta(0)=0,\quad \phi(0)=1 \qquad at \quad \eta=0\\ &f'(\eta)\to 0,\quad g(\eta)\to 0,\quad \theta(\eta)\to 0,\quad \phi(\eta)\to 0 \qquad as \quad \eta\to\infty \end{aligned} \tag{15}$$

The significant parameters are specified in the equations that do not include proportions.

$$\begin{aligned} &M=\frac{\sigma B_0^2}{\rho a},\ \mathrm{Pr}=\frac{\nu}{\alpha}=\frac{\nu\rho C_p}{k},\ L_e=\frac{\alpha}{D_B},\ Q=\frac{Q_0}{a\rho C_p},\ Gr_x=\frac{g_c\beta_T\left(T_w-T_\infty\right)}{a^2x},\\ &N_b=\frac{\tau D_B\left(C_w-C_\infty\right)}{\nu},\quad N_t=\frac{\tau D_T\left(T_w-T_\infty\right)}{\nu},\ Gr_c=\frac{g_c\beta_C\left(C_w-C_\infty\right)}{a^2x},\\ &R=\frac{16\sigma_1T_\infty^3}{3kk^*},K_E=\frac{k_r^2}{a},E=\frac{E_a}{KT_\infty},Du=\frac{D_Mk_T\left(C_w-C_\infty\right)}{C_SC_p\nu a^2\left(T_w-T_\infty\right)},\ \mathrm{Re}^2=\frac{ax^2}{\nu} \end{aligned} \tag{16}$$

3. Physical Quantities of Interests

The relevant physical parameters that have an impact on the flow are the local skin friction coefficient in the direction of x Cf_x and the direction of z Cf_z, the local Nusselt number Nux, and the local Sherwood number Sh_x. The following explanations apply to these numerical values

$$C\,f_x=\frac{2\tau_{wx}}{\rho\left(ax\right)^2},\ Cf_z=\frac{2\tau_{wz}}{\rho\left(ax\right)^2},\ Nu_x=\frac{xq_w}{k\left(T_w-T_\infty\right)},\ Sh_x=\frac{x\,j_w}{D_B\left(C_w-C_\infty\right)} \tag{17}$$

where τwx, τwy, qw and jw are the wall skin friction, wall heat flux and wall mass flux respectively given by

$$\tau_{wx} = \mu\left[\frac{\partial u}{\partial y}\right]_{y=0}, \quad \tau_{wz} = \mu\left[\frac{\partial w}{\partial y}\right]_{y=0}, \quad q_w = -k\left[\frac{\partial T}{\partial y}\right]_{y=0}, \quad j_w = -D_B\left[\frac{\partial C}{\partial y}\right]_{y=0} \tag{18}$$

The following is an expression of the factor of skin friction, the Nusselt number, and the Sherwood number in their non-dimensional forms concerning the similarity component

$$\mathrm{Re}_x^{1/2}\, Cf_x = 2f''(0), \quad \mathrm{Re}_x^{1/2}\, Cf_z = 2g'(0), \quad \mathrm{Re}_x^{1/2}\, Nu_x = -(1+R)\theta'(0), \quad \mathrm{Re}_x^{1/2}\, Sh_x = -\phi'(0) \tag{19}$$

4. Solution Methodology

The non-linear ODE system (11–14), susceptible to constraints 15, was solved using the shooting technique for various values of the related parameters. We were able to figure out from the graphs that the behavior of the solutions does not change much when the value is greater than 8. Because of this, and based on the results of the computational experiments described above, we are considering using the range [0, 8] as the domain of the issue rather than the range [0,∞]. We denote f by y_1, g by y_4, θ by y_6, and ϕ by y_8 for converting the boundary value problem (11-15) to the following initial value problem of 9 first-order differential equations.

$$y_1' = y_2,$$

$$y_2' = y_3,$$

$$y_3' = \frac{1}{\left(1+\frac{1}{\beta}\right)}\left(-y_1y_3 + y_2^2 - Gr_x y_6 + Gr_c y_8 + \frac{M}{1+m^2}\left(y_2 + my_4\right)\right)$$

$$y_4' = y_5,$$

$$y_5' = \frac{1}{\left(1+\frac{1}{\beta}\right)}\left(y_2y_4 - y_1y_5 - Gr_x y_6 + Gr_c y_8 - \frac{M}{1+m^2}\left(-y_4 + my_2\right)\right),$$

$$y_6' = y_7,$$

$$y_7' = \frac{1}{(1+R\,\mathrm{Pr})}\left(-\mathrm{Pr}\, y_1y_7 - \mathrm{Pr}\, N_b\left(y_9y_7 + \frac{N_t}{N_b}y_7^{\,2}\right) - \mathrm{Pr}\, Qy_6 - \mathrm{Pr}\, D_u y_9\right),$$

$$y_8' = y_9,$$

$$y_{10}' = -\mathrm{Pr}\, L_e\, y_1\, y_9 - \frac{N_t}{N_b}y_7' + y_8K_E\left(1+y_6\right)^m \exp\left(\frac{-E}{1+y_6}\right)$$

5. Results and Discussion

Plotting Figure 2 to Figure 27 allows one to see the influence that several different physical factors have on the tangential velocity $f^{i}(\eta)$, the transverse velocity g(η), the nanoparticle concentration ϕ (η), and the temperature θ(η) profiles. In each and every one of these calculations, unless it was specifically stated differently, we assumed that Nb = 0.3, Nt = 0.7, P r = 0.71, Le = 0.6, = 0.5, M = 0.5, m = 0.2, Gr = 0.5, Gm = 0.5, Q0 = 0.5, R = 1, E = 0.5, Du=0.5.

The influence of the magnetic parameter M on the tangential velocity f'(η), longitudinal velocity g(η), temperature θ(η), and concentration ϕ(η) profiles, respectively, is shown in Figure 2 through Figure 5. The velocity profile f'(η) drops as the values of M rise, and a similar trend has been seen with the transverse velocity profile g(η). On the other hand, the temperature profile θ(η) and the concentration profile ϕ(η) increase as M grows. When M is increased, a force of drag known as the Lorentz force also rises. As a result of the fact that this force works against the flow of nanofluid, the velocity in the direction of the flow slows down. In addition, since an electrically conducting nanofluid and a strong magnetic field in an order that is orthogonal to the flow are being examined, an increase in M will result in an increase in the force in the z-direction, which will lead to a decrease in the longitudinal velocity profile g(η).

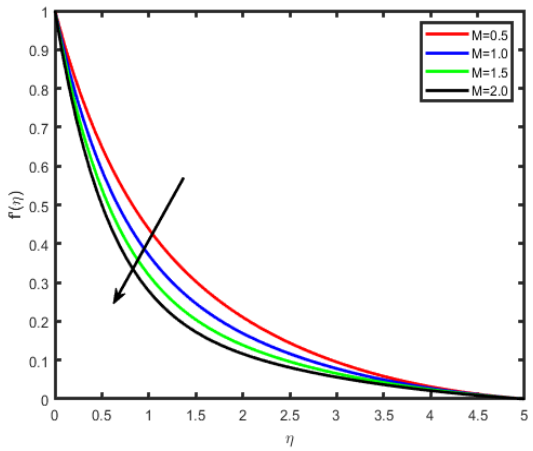

Fig. 2. Influence of M on f′(n)

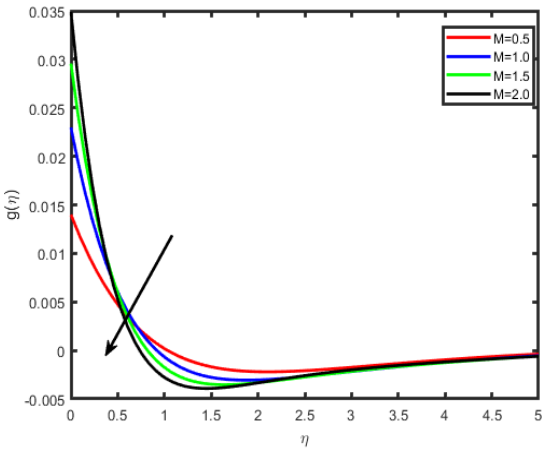

Fig. 3. Contribution of M on g(n)

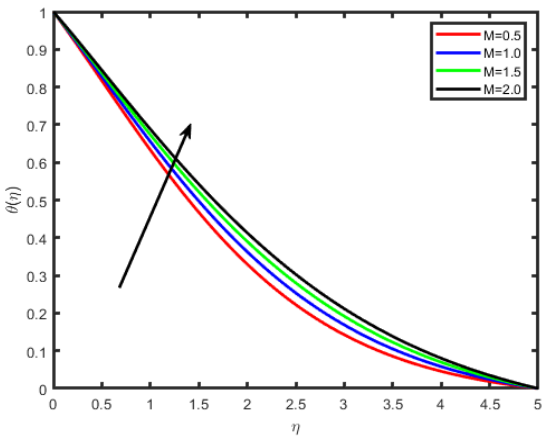

Fig. 4. Effect of M on θ(n)

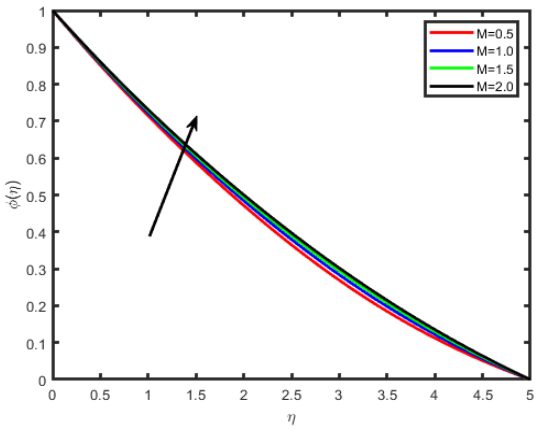

Fig. 5. Effect of M on φ (n)

The effects of the Hall component m on the tangential velocity $f^{i}(\eta)$, transverse velocity g(η), nanoparticle concentration ϕ(η), and temperature θ(η) patterns are depicted in Figure 6 to Figure 9 accordingly. As m becomes higher, it can be seen in Figure 6 and Figure 7 that the velocity f'(η) and g(η) profiles go higher as well. On the other hand, Figure 8 and Figure 9 shows that both the

temperature and concentration curves drop as the distance m increases. This is because the enclosure of the Hall parameter has the effect of decreasing the effective conductivity, resulting in a diminishing of the resistive force induced by the magnetic field. Therefore, an increase in the Hall factor increases the velocity component.

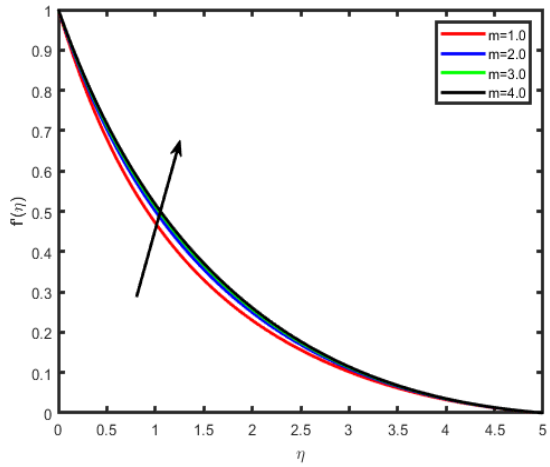

Fig. 6. Influence of m on f′(n)

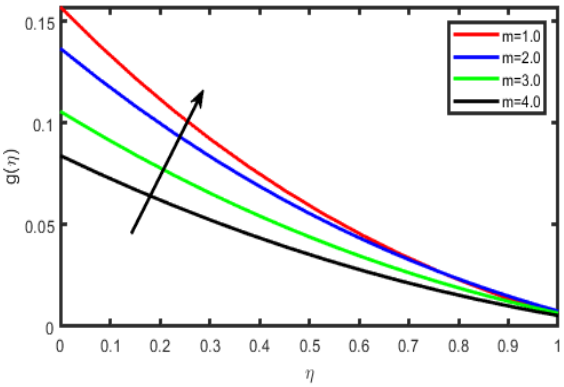

Fig. 7. Contribution of m on g(n)

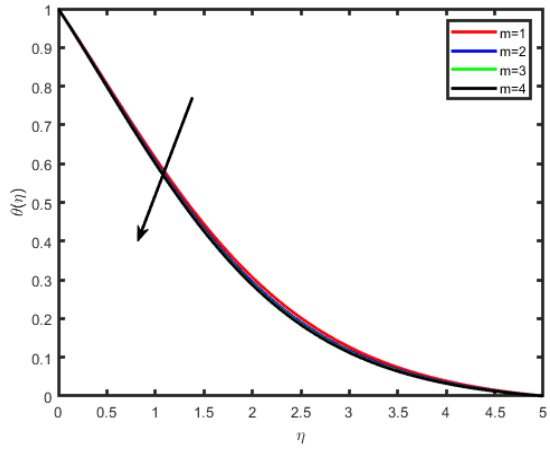

Fig. 8. Effect of m on θ(n)

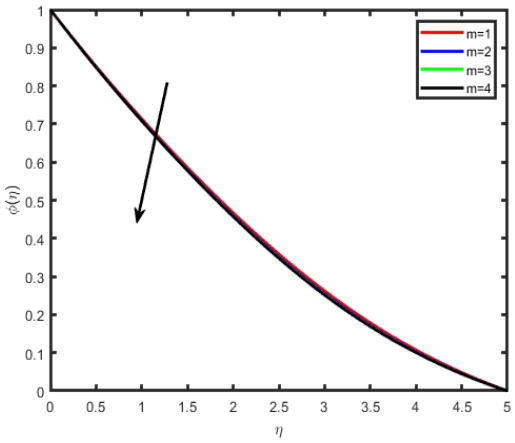

Fig. 9. Influence of m on φ (n)

The influence that the Casson component (β) has on the velocity outline is seen in Figure 10 and Figure 11. It has come to our attention that as it grows, the velocity and the thickness of the boundary layer decrease. Therefore, the magnitude of the velocity is more significant in Casson fluid as contrasted to viscous fluids since the Casson fluid is less dense. The consequences of the thermal Grashof Gr numeral and the mass Grashof Gm numeral on the tangential velocity f"(η) and the transverse velocity g(η) are correspondingly portrayed in Figure 12 to Figure 15. The Grashof numeral is a ratio of the buoyant force to the viscous force. Because it is assembled as a result of the natural convection flow, it indicates an increase in both the tangential and transverse velocities of the liquid. This occurs because a more significant Grashof number advances a more vital buoyancy force, which in turn means a higher flow movement.

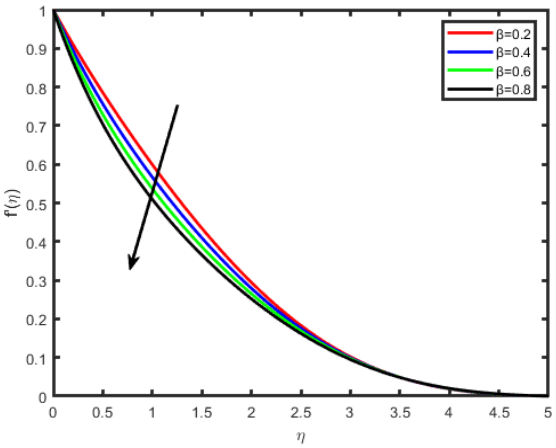

Fig. 10. Influence of β on f′(n)

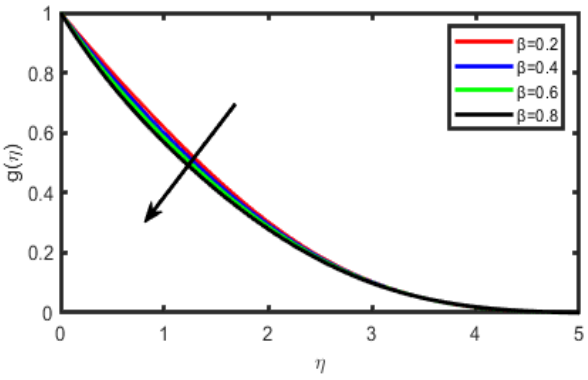

Fig. 11. Contribution of m on g(n)

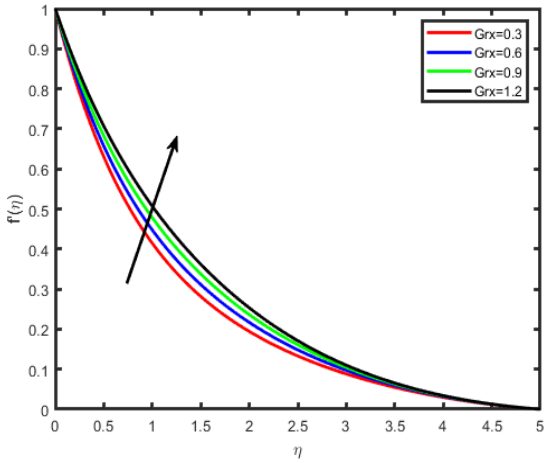

Fig. 12. Influence of Gr on f′(n)

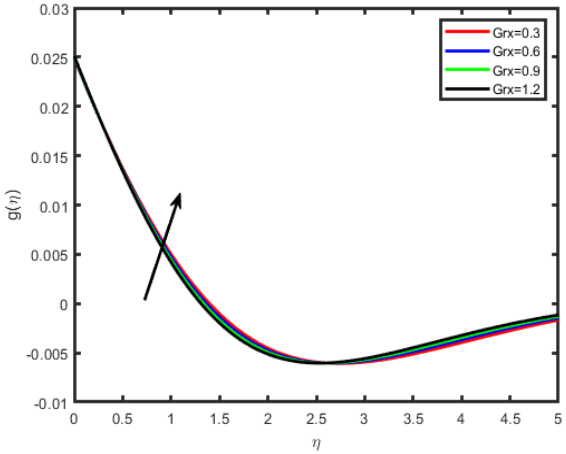

Fig. 13. Contribution of Gr on g(n)

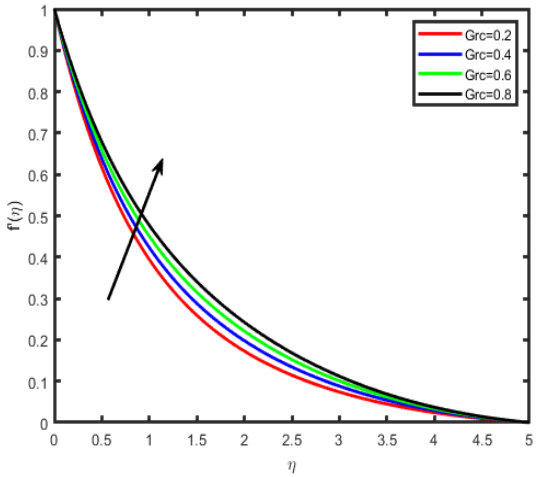

Fig. 14. Influence of Gm on f′(n)

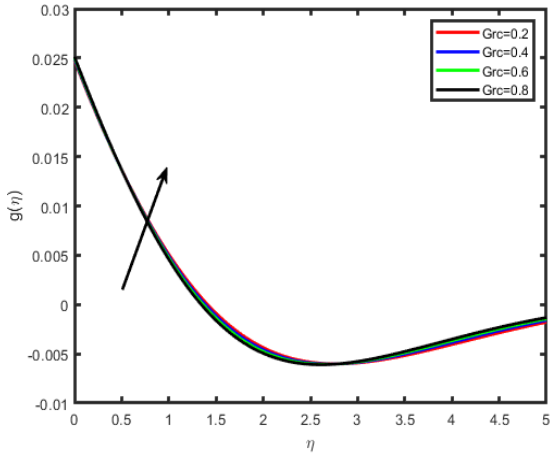

Fig. 15. Contribution of Gm on g(n)

The distribution of the thermal radiation factor R, and Diffusion thermo parameter (Du) on temperature sector as seen in Figure 16 and Figure 17. It is interesting to note that a higher value of R strengthens the temperature. This is because the radiation criterion generates thermal energy in the flow region; as a result, enhancements have been seen in the temperature field. As the Dufour parameter increases, the energy or temperature profiles increases. The Dufour number denotes the

contribution of the concentration gradients to the thermal energy flux in the flow. It can be seen that an increase in the Dufour number causes a rise in temperature.

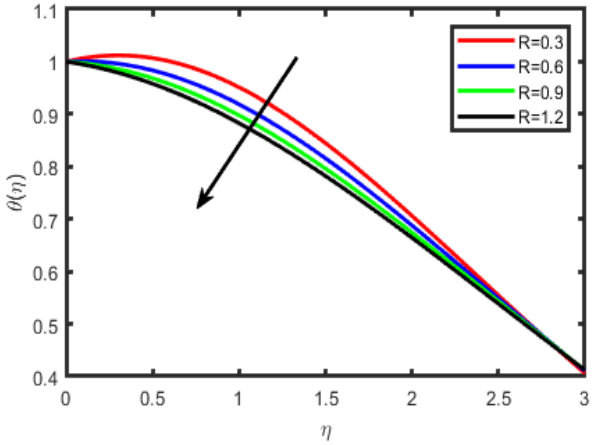

Fig. 16. Effect of R on θ(n)

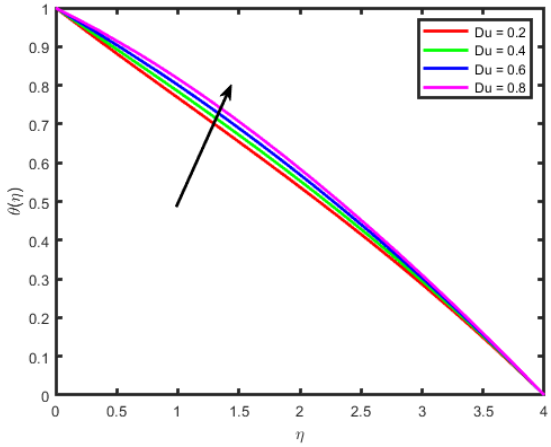

Fig. 17. Influence of Du on θ(η)

Figure 18 demonstrates that an elevation in the resistance of the heat source or sink causes an increase in the temperature. This is because an increase in the resistance of heat production causes the temperature to rise. When it comes to focusing, one might expect to see the exact opposite behavior (Figure 19). Figure 20 and Figure 21 provide a study that analyzes the Brownian motion parameter Nb's effect on the temperature and concentration curves. Based on these statistics, we can deduce that an increase in the values of Nb produces a drop in the nanoparticle concentration profile while simultaneously increasing temperature. The Brownian motion refers to the random movement of nanoparticles immersed in a fluid. This motion is induced by the collision of nanoparticles with the particles that make up the fluid. An increase in the thermophoretic effect leads to an increase in the Brownian motion effect, which produces a rise in temperature due to increased kinetic energy.

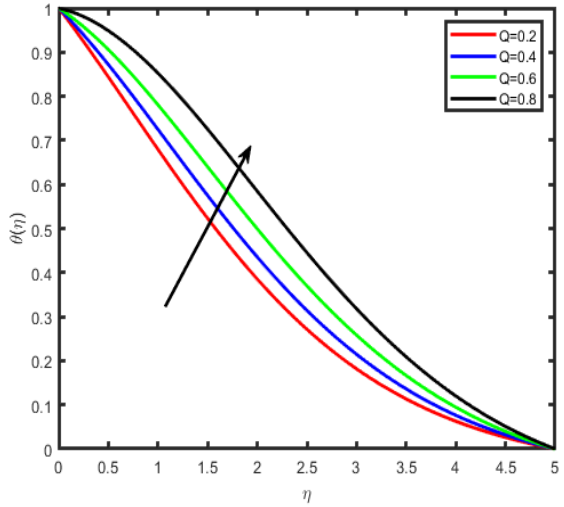

Fig. 18. Effect of Q on θ(n)

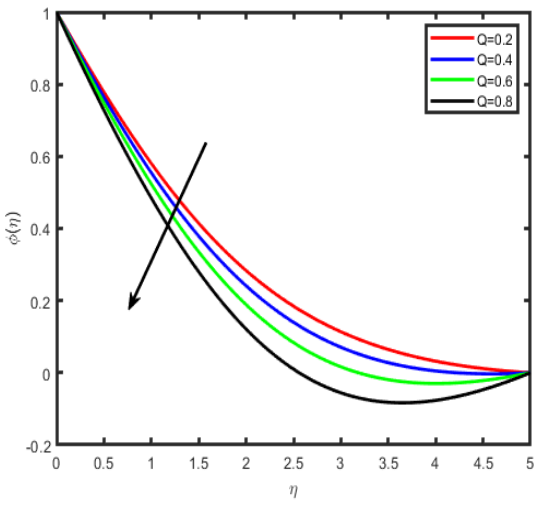

Fig. 19. Influence of Q on φ(n)

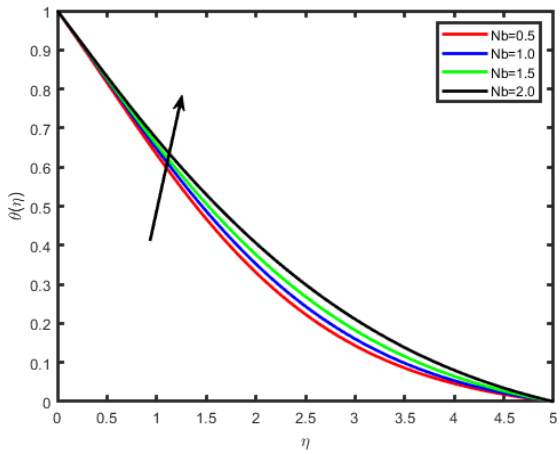

Fig. 20. Effect of Nb on θ(n)

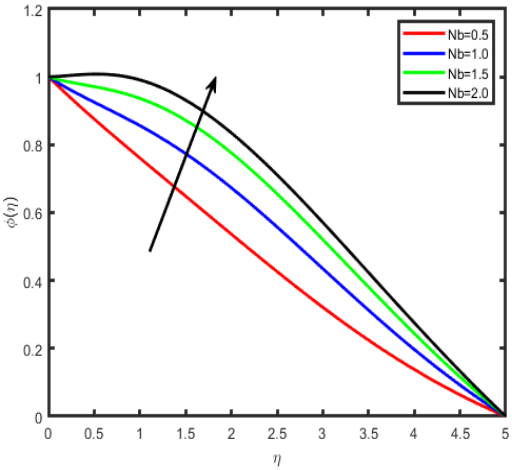

Fig. 21. Influence of Nb on φ(n)

The influence of the thermophoresis parameter Nt on the temperature and the nanoparticles concentration profile is shown in Figure 22 and Figure 23, respectively. When there is a rise in Nt, it is possible to notice an increase in the temperature and concentration fields. The thermophoresis parameter is responsible for a substantial part of the flow of heat transfer. When Nt is raised, the thermophoresis force increases, transporting nanoparticles from the hot zone to the cold region. As a consequence of this movement, the boundary layer's temperature, and thickness rise. The Lewis number (Le) influence may be seen in Figure 24 and Figure 25, which depict the temperature and nanoparticle concentration trends, respectively. It has been shown that increasing Le results in a temperature rise while increasing the Lewis number results in a drop in concentration. The influence of the activation energy (E) on the concentration field is seen in Figure 26. The graph demonstrates that the concentration profile rises as the value of E increases. The Arrhenius function degrades due to the activation energy snowballing value, which ultimately leads to the encouragement of the generative chemical reaction, which in turn causes an improvement in the concentration field. When the temperature is low and the activation energy is high, a lower reaction rate constant is produced, which causes the chemical reaction to proceed more slowly. Increased focus is the direct result of this strategy. Figure 27 demonstrates that an increase in the rate of chemical reaction (σ) causes a significant decrease in the concentration profile. A high chemical reaction rate causes a fallout solute boundary layer to become denser.

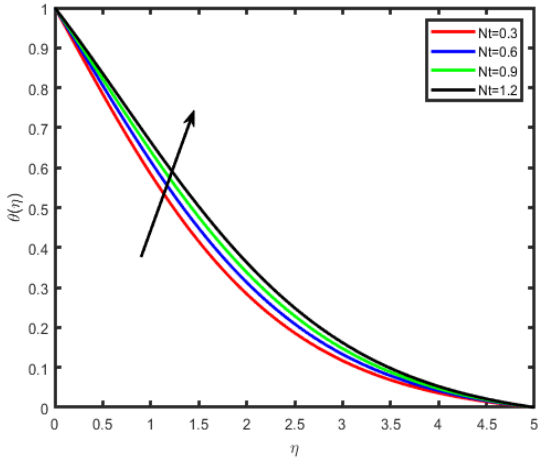

Fig. 22. Effect of Nt on θ(n)

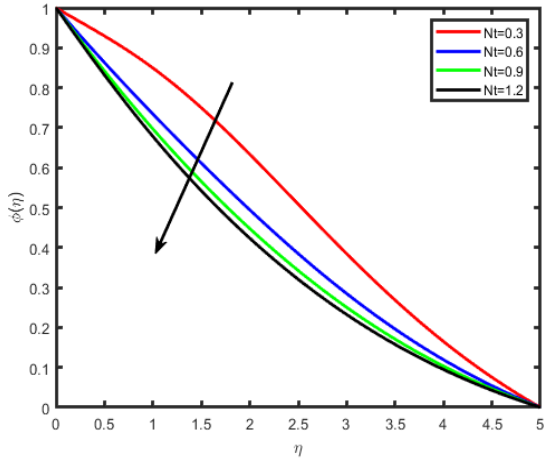

Fig. 23. Influence of Nt on φ(n)

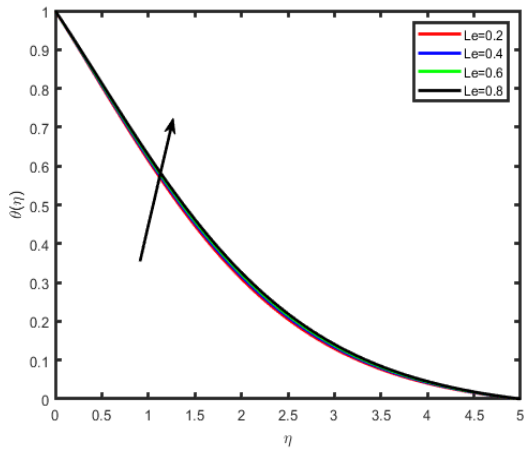

Fig. 24. Effect of Le on θ(n)

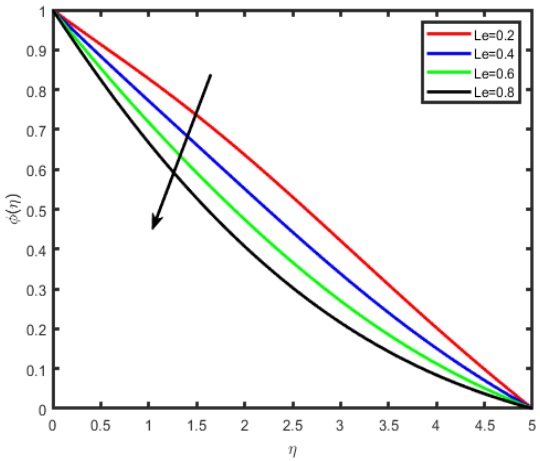

Fig. 25. Influence of Le on φ(n)

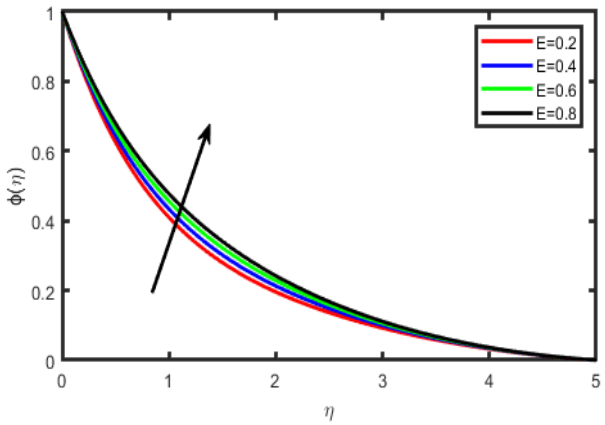

Fig. 26. Influence of E on φ(n)

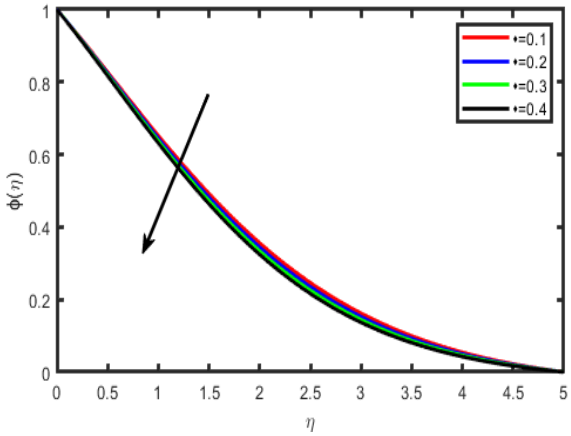

Fig. 27. Influence of σ on φ(n)

In Table 1, we summarize the effects of various material factors on the local Sherwood numeral, skin friction factor, and local Nusselt numeral. These mathematical results are achieved for the following values of Nb = 0.3, β=0.5, Nt = 0.7, Pr = 0.71, Le = 0.6, M = 0.5, m = 0.2, Gr = 0.5, Gm = 0.5, Q = 0.5, and R = 1. It has been seen that the skin-friction coefficient in the x directive decreases with an increase in the thermal Grashof number Gr, the mass Grashoff number Gm, the Hall current factor m, and the Brownian motion factor Nb. On the other hand, it advances with an expansion in the value of the magnetic factor M, the heat source factor, the radiation, the Prandtl number Pr, and the thermophoresis parameter Nt. In the z-direction, the coefficient of the skin's friction behaves differently than in any other direction. When the value of the Hall current parameter m, the thermal Grashof number, the mass Grashoff number, and the Prandtl number all increase, the Nusselt number goes up; regardless, it goes down when the value of the magnetic field parameter M, the heat source factor, and the radiation factor are all increased. The Sherwood numeral exhibits an increasing behavior for the thermal Grashof numeral Gr, the magnetic field factor M, the Brownian motion factor Nb, the heat source and radiation factor, and the thermophoresis parameter Nt, whereas the Grashoff numeral Gm and Prandtl number exhibit a decreasing behavior.

As part of the process to validate the numerical approach that was used, the results were compared to those that had been achieved in the past by Suresh Kumar *et al.,* [7] for a variety of parameter values, and the result reveals that there is a good concordance, as can be seen in Table 2.

Table 1
Numerical values of $\mathrm{Re}_x^{1/2} Cf_x$, $\mathrm{Re}_x^{1/2} Cf_z$, $\mathrm{Re}_x^{1/2} Nu_x$, $\mathrm{Re}_x^{1/2} Sh_x$

Gr	Gm	Q	m	Nb	R	M	Pr	Nt	-2f"(0)	-2g'(0)	-θ'(0)	-ϕ'(0)
0.5									1.28476	0.852112	0.521275	0.9514666
1.0									0.99786	0.912543	0.532396	0.9916275
1.5									0.73544	0.954295	0.545753	1.0249678
	0.3								0.987521	0.851283	0.503213	0.1747477
	0.6								0.84755	0.985284	0.512408	0.1126548
	0.9								0.71257	1.252193	0.578594	0.2756178
			1						1.52148	0.852157	0.314535	0.8857502
			2						1.02144	0.954796	0.297895	0.7952024
			3						0.81254	0.998502	0.231283	0.9458266
				0.2					0.95123	0.952158	0.845278	0.5850575
				0.4					0.81522	0.961202	0.821507	0.6128604
				0.6					0.71251	0.985284	0.803264	0.6972754
						0.5			0.94526	1.025494	0.987573	0.7859567
						1.0			1.24548	0.985205	0.912524	0.8952854
						1.5			1.40358	0.8512921	0.895207	0.9452954
							0.6		0.97857	1.0214497	0.125494	0.9878670
							0.71		0.91206	0.9852349	0.157853	0.9459548
							0.76		0.84525	0.9032495	0.198723	0.923857
								0.3	1.54524	0.9852855	0.854286	0.5120555
								0.6	1.12546	0.9120948	0.812553	0.5929858
								0.9	0.87528	0.89622378	0.752196	0.612968
		0.2							0.712490	0.9875763	0.954224	0.9857589
		0.4							0.78528	0.9452254	0912507	0.9744856
		06							0.81257	0.9132683	0.865795	0.96490487
					0.5				0.87526	1.0875465	0.745236	0.984724
					1.0				0.89525	0.9442366	0.736557	0.918570
					1.5				0.91254	0.9114367	0.715407	0.9109568

Table 2
Comparison of −θ' (0) for various values of Pr when Nb= 0.3, Nt= 0.7, Pr= 0.71, Le = 0.6, M= 0.5, Gr = 0.5, Gm= 0.5, m=0.2, Q=0.5, R=1, β=0, Du=0

Pr	Suresh Kumar *et al.,* [7]	Present values
0.01	0.019125	0.0181545
0.72	0.807785	0.8737634
1	1.000000	1.0013333
3	1.924785	1.9645345
10	3.732452	3.8264e72

6. Conclusion

In the present research, the impact of the Hall current Diffusion thermo and Activation energy on heat and mass transfer of nanofluid flowing over a linearly stretching sheet in the presence of thermal radiation and heat source/ sink is addressed. The main achievements have been summarized as follows.

i. The temperature θ(η) of the fluid is enhanced while increasing the thermophoresis parameter Nt and the Brownian motion parameter Nb.
ii. As the Casson fluid parameter (β) increases, there is a corresponding decrease in the fluid's resultant velocity.

iii. The temperature rises with the values of the heat source/sink parameter (Q), Diffusion thermo Parameter (Du) and the Brownian motion parameter (Nb), yet the concentration profile of nanoparticles falls. On the other hand, the radiation parameter was shown to have the opposite tendency (R).
iv. Raising the Prandtl number (Pr) tends to bring about a decrease in both the temperature and concentration profiles.
v. A rise in Le causes an increase in temperature, but an increase in Lewis number causes a drop in concentration.
vi. When the hall parameter (m) is increased, the velocity increases, but the opposite trend is shown when temperature and concentration are considered.

References

[1] Al-Khaled, Kamel, and Sami Ullah Khan. "Thermal aspects of casson nanoliquid with gyrotactic microorganisms, temperature-dependent viscosity, and variable thermal conductivity: bio-technology and thermal applications." *Inventions* 5, no. 3 (2020): 39. https://doi.org/10.3390/inventions5030039
[2] Ali, Bagh, Rizwan Ali Naqvi, Amir Haider, Dildar Hussain, and Sajjad Hussain. "Finite element study of mhd impacts on the rotating flow of casson nanofluid with the double diffusion Cattaneo-Christov heat flux model." *Mathematics* 8, no. 9 (2020): 1555. https://doi.org/10.3390/math8091555
[3] Ghosh, Riya, Titilayo M. Agbaje, Sabyasachi Mondal, and Sachin Shaw. "Bio-convective viscoelastic Casson nanofluid flow over a stretching sheet in the presence of induced magnetic field with Cattaneo-Christov double diffusion." *International Journal of Biomathematics* 15, no. 03 (2022): 2150099. https://doi.org/10.1142/S1793524521500996
[4] Wang, Fuzhang, Juan Zhang, Salem Algarni, Muhammad Naveed Khan, Talal Alqahtani, and Shafiq Ahmad. "Numerical simulation of hybrid Casson nanofluid flow by the influence of magnetic dipole and gyrotactic microorganism." *Waves in Random and Complex Media* (2022): 1-16. https://doi.org/10.1080/17455030.2022.2032866
[5] Prasad, Kerehalli Vinayaka, Hanumesh Vaidya, Fateh Mebarek Oudina, Khalid Mustafa Ramadan, Muhammad Ijaz Khan, Rajashekhar Choudhari, Rathod Kirankumar Gulab, Iskander Tlili, Kamel Guedri, and Ahmed M. Galal. "Peristaltic activity in blood flow of Casson nanoliquid with irreversibility aspects in vertical non-uniform channel." *Journal of the Indian Chemical Society* 99, no. 8 (2022): 100617. https://doi.org/10.1016/j.jics.2022.100617
[6] Li, Shuguang, Kodi Raghunath, Ayman Alfaleh, Farhan Ali, A. Zaib, M. Ijaz Khan, Sayed M. ElDin, and V. Puneeth. "Effects of activation energy and chemical reaction on unsteady MHD dissipative Darcy-Forchheimer squeezed flow of Casson fluid over horizontal channel." *Scientific Reports* 13, no. 1 (2023): 2666. https://doi.org/10.1038/s41598-023-29702-w
[7] Suresh Kumar, Y., Shaik Hussain, K. Raghunath, Farhan Ali, Kamel Guedri, Sayed M. Eldin, and M. Ijaz Khan. "Numerical analysis of magnetohydrodynamics Casson nanofluid flow with activation energy, Hall current and thermal radiation." *Scientific Reports* 13, no. 1 (2023): 4021. https://doi.org/10.1038/s41598-023-28379-5
[8] Raghunath, Kodi, Obulesu Mopuri, Sujatha Sree, and Venkateswaraju Konduru. "Investigation of MHD Casson fluid flow past a vertical porous plate under the influence of thermal diffusion and chemical reaction." *Heat Transfer* 51, no. 1 (2022): 377-394. https://doi.org/10.1002/htj.22311
[9] Raghunath, Kodi, and Obulesu Mopuri. "Unsteady MHD oscillatory Casson fluid flow past an inclined vertical porous plate in the presence of chemical reaction with heat absorption and Soret effects." *Heat Transfer* 51, no. 1 (2022): 733-752. https://doi.org/10.1002/htj.22327
[10] Vaddemani, Ramachandra Reddy, Raghunath Kodi, and Obulesu Mopuri. "Characteristics of MHD Casson fluid past an inclined vertical porous plate." *Materials Today: Proceedings* 49 (2022): 2136-2142. https://doi.org/10.1016/j.matpr.2021.08.328
[11] Choi, S. US, and Jeffrey A. Eastman. *Enhancing thermal conductivity of fluids with nanoparticles*. No. ANL/MSD/CP-84938; CONF-951135-29. Argonne National Lab.(ANL), Argonne, IL (United States), 1995.
[12] Eastman, Jeffrey A., S. U. S. Choi, Sheng Li, W. Yu, and L. J. Thompson. "Anomalously increased effective thermal conductivities of ethylene glycol-based nanofluids containing copper nanoparticles." *Applied Physics Letters* 78, no. 6 (2001): 718-720. https://doi.org/10.1063/1.1341218
[13] Ahmad, Shafiq, and Sohail Nadeem. "Analysis of activation energy and its impact on hybrid nanofluid in the presence of Hall and ion slip currents." *Applied Nanoscience* 10 (2020): 5315-5330. https://doi.org/10.1007/s13204-020-01334-w

[14] Ahmad, Shafiq, Muhammad Naveed Khan, and Sohail Nadeem. "Unsteady three dimensional bioconvective flow of Maxwell nanofluid over an exponentially stretching sheet with variable thermal conductivity and chemical reaction." *International Journal of Ambient Energy* 43, no. 1 (2022): 6542-6552. https://doi.org/10.1080/01430750.2022.2029765

[15] Hou, Enran, Fuzhang Wang, Muhammad Naveed Khan, Shafiq Ahmad, Aysha Rehman, Abdulrazak H. Almaliki, El-Sayed M. Sherif, Ahmed M. Galal, and Maram S. Alqurashi. "Flow analysis of hybridized nanomaterial liquid flow in the existence of multiple slips and hall current effect over a slendering stretching surface." *Crystals* 11, no. 12 (2021): 1546. https://doi.org/10.3390/cryst11121546

[16] Ahmad, Shafiq, Sohail Nadeem, and Muhammad Naveed Khan. "Heat enhancement analysis of the hybridized micropolar nanofluid with Cattaneo-Christov and stratification effects." *Proceedings of the Institution of Mechanical Engineers, Part C: Journal of Mechanical Engineering Science* 236, no. 2 (2022): 943-955. https://doi.org/10.1177/09544062211010833

[17] Ahmad, Shafiq, and Sohail Nadeem. "Thermal analysis in buoyancy driven flow of hybrid nanofluid subject to thermal radiation." *International Journal of Ambient Energy* 43, no. 1 (2022): 3868-3876. https://doi.org/10.1080/01430750.2020.1861090

[18] Khan, Muhammad Naveed, Sohail Nadeem, Shafiq Ahmad, and Anber Saleem. "Mathematical analysis of heat and mass transfer in a Maxwell fluid." *Proceedings of the Institution of Mechanical Engineers, Part C: Journal of Mechanical Engineering Science* 235, no. 20 (2021): 4967-4976. https://doi.org/10.1177/0954406220976704

[19] Shah, Zahir, and Asad Ullah. "Ferrofluid treatment with insertion of electric field inside a porous cavity considering forced convection." *Waves in Random and Complex Media* (2023): 1-19. https://doi.org/10.1080/17455030.2023.2169386

[20] Shah, Zahir, Muhammad Rooman, and Meshal Shutaywi. "Computational analysis of radiative engine oil-based Prandtl-Eyring hybrid nanofluid flow with variable heat transfer using the Cattaneo-Christov heat flux model." *RSC Advances* 13, no. 6 (2023): 3552-3560. https://doi.org/10.1039/D2RA08197K

[21] Tang, Tao-Qian, Muhammad Rooman, Zahir Shah, Muhammad Asif Jan, Narcisa Vrinceanu, and Mihaela Racheriu. "Computational study and characteristics of magnetized gold-blood Oldroyd-B nanofluid flow and heat transfer in stenosis narrow arteries." *Journal of Magnetism and Magnetic Materials* 569 (2023): 170448. https://doi.org/10.1016/j.jmmm.2023.170448

[22] Asghar, Adnan, Abdul Fattah Chandio, Zahir Shah, Narcisa Vrinceanu, Wejdan Deebani, Meshal Shutaywi, and Liaquat Ali Lund. "Magnetized mixed convection hybrid nanofluid with effect of heat generation/absorption and velocity slip condition." *Heliyon* 9, no. 2 (2023). https://doi.org/10.1016/j.heliyon.2023.e13189

[23] Khan, Imtiaz, Muhammad Asif Zahoor Raja, Muhammad Abdul Rehman Khan, Muhammad Shoaib, Saeed Islam, and Zahir Shah. "Design of backpropagated intelligent networks for nonlinear second-order Lane-Emden pantograph delay differential systems." *Arabian Journal for Science and Engineering* 47, no. 2 (2022): 1197-1210. https://doi.org/10.1007/s13369-021-05814-1

[24] AlDosari, Sahar Mohammed, Saeed Banawas, Hevi Seerwan Ghafour, Iskander Tlili, and Quynh Hoang Le. "Drug release using nanoparticles in the cancer cells on 2-D materials in order to target drug delivery: A numerical simulation via molecular dynamics method." *Engineering Analysis with Boundary Elements* 148 (2023): 34-40. https://doi.org/10.1016/j.enganabound.2022.12.020

[25] Aljaloud, Amjad Salamah M., Leila Manai, and Iskander Tlili. "Bioconvection flow of Cross nanofluid due to cylinder with activation energy and second order slip features." *Case Studies in Thermal Engineering* 42 (2023): 102767. https://doi.org/10.1016/j.csite.2023.102767

[26] Raghunath, Kodi. "Study of Heat and Mass Transfer of an Unsteady Magnetohydrodynamic (MHD) Nanofluid Flow Past a Vertical Porous Plate in the Presence of Chemical Reaction, Radiation and Soret Effects." *Journal of Nanofluids* 12, no. 3 (2023): 767-776. https://doi.org/10.1166/jon.2023.1965

[27] Bafakeeh, Omar T., Kodi Raghunath, Farhan Ali, Muhammad Khalid, El Sayed Mohamed Tag-ElDin, Mowffaq Oreijah, Kamel Guedri, Nidhal Ben Khedher, and Muhammad Ijaz Khan. "Hall current and Soret effects on unsteady MHD rotating flow of second-grade fluid through porous media under the influences of thermal radiation and chemical reactions." *Catalysts* 12, no. 10 (2022): 1233. https://doi.org/10.3390/catal12101233

[28] Raghunath, Kodi, and Ravuri Mohanaramana. "Hall, Soret, and rotational effects on unsteady MHD rotating flow of a second-grade fluid through a porous medium in the presence of chemical reaction and aligned magnetic field." *International Communications in Heat and Mass Transfer* 137 (2022): 106287. https://doi.org/10.1016/j.icheatmasstransfer.2022.106287

[29] Tlili, Iskander, and Thamer Alharbi. "Investigation into the effect of changing the size of the air quality and stream to the trombe wall for two different arrangements of rectangular blocks of phase change material in this wall." *Journal of Building Engineering* 52 (2022): 104328. https://doi.org/10.1016/j.jobe.2022.104328

[30] Dero, Sumera, T. N. Abdelhameed, Kamel Al-Khaled, Liaquat Ali Lund, Sami Ullah Khan, and Iskander Tlili. "Contribution of suction phenomenon and thermal slip effects for radiated hybrid nanoparticles (Al_2O_3-Cu/H_2O) with stability framework." *International Journal of Modern Physics* B (2022): 2350147. https://doi.org/10.1142/S0217979223501473

[31] Banawas, Saeed, Talib K. Ibrahim, Iskander Tlili, and Quynh Hoang Le. "Reinforced Calcium phosphate cements with zinc by changes in initial properties: A molecular dynamics simulation." *Engineering Analysis with Boundary Elements* 147 (2023): 11-21. https://doi.org/10.1016/j.enganabound.2022.11.033

[32] Aljaloud, Amjad Salamah M., Kamel Smida, Hawzhen Fateh M. Ameen, M. A. Albedah, and Iskander Tlili. "Investigation of phase change and heat transfer in water/copper oxide nanofluid enclosed in a cylindrical tank with porous medium: A molecular dynamics approach." *Engineering Analysis with Boundary Elements* 146 (2023): 284-291. https://doi.org/10.1016/j.enganabound.2022.10.034

[33] Deepthi, V. V. L., Maha MA Lashin, N. Ravi Kumar, Kodi Raghunath, Farhan Ali, Mowffaq Oreijah, Kamel Guedri, El Sayed Mohamed Tag-ElDin, M. Ijaz Khan, and Ahmed M. Galal. "Recent development of heat and mass transport in the presence of Hall, ion slip and thermo diffusion in radiative second grade material: application of micromachines." *Micromachines* 13, no. 10 (2022): 1566. https://doi.org/10.3390/mi13101566

[34] Ganjikunta, Aruna, Hari Babu Kommaddi, Venkateswarlu Bhajanthri, and Raghunath Kodi. "An unsteady MHD flow of a second-grade fluid passing through a porous medium in the presence of radiation absorption exhibits Hall and ion slip effects." *Heat Transfer* (2023). https://doi.org/10.1002/htj.22716

[35] Kodi, Raghunath, Mohanaramana Ravuri, Nagesh Gulle, Charankumar Ganteda, Sami Ullah Khan, and M. Ijaz Khan. "Hall and ion slip radiative flow of chemically reactive second grade through porous saturated space via perturbation approach." *Waves in Random and Complex Media* (2022): 1-17. https://doi.org/10.1080/17455030.2022.2108555

[36] Rajakarunakaran, Surya Abisek, Arun Raja Lourdu, Suresh Muthusamy, Hitesh Panchal, Ali Jawad Alrubaie, Mustafa Musa Jaber, Mohammed Hasan Ali et al. "Prediction of strength and analysis in self-compacting concrete using machine learning based regression techniques." *Advances in Engineering Software* 173 (2022): 103267. https://doi.org/10.1016/j.advengsoft.2022.103267

[37] Bai, Jie, Dler Hussein Kadir, Moram A. Fagiry, and Iskander Tlili. "Numerical analysis and two-phase modeling of water Graphene Oxide nanofluid flow in the riser condensing tubes of the solar collector heat exchanger." *Sustainable Energy Technologies and Assessments* 53 (2022): 102408. https://doi.org/10.1016/j.seta.2022.102408

[38] Okonkwo, Paul C., Ikram Ben Belgacem, Manaf Zghaibeh, and Iskander Tlili. "Optimal sizing of photovoltaic systems based green hydrogen refueling stations case study Oman." *International Journal of Hydrogen Energy* 47, no. 75 (2022): 31964-31973. https://doi.org/10.1016/j.ijhydene.2022.07.140

[39] Reddy, Yanala Dharmendar, Dodda Ramya, and Laxmianarayanagari Anand Babu. "Effect of thermal radiation on MHD boundary layer flow of nanofluid and heat transfer over a non-linearly stretching sheet with transpiration." *Journal of Nanofluids* 5, no. 6 (2016): 889-897. https://doi.org/10.1166/jon.2016.1284

[40] Kothandapani, M., and J. Prakash. "Effects of thermal radiation parameter and magnetic field on the peristaltic motion of Williamson nanofluids in a tapered asymmetric channel." *International Journal of Heat and Mass Transfer* 81 (2015): 234-245. https://doi.org/10.1016/j.ijheatmasstransfer.2014.09.062

[41] Sulochana, C., S. Payad Samrat, and N. Sandeep. "Thermal radiation effect on MHD nanofluid flow over a stretching sheet." In *International Journal of Engineering Research in Africa*, vol. 23, pp. 89-102. Trans Tech Publications Ltd, 2016. https://doi.org/10.4028/www.scientific.net/JERA.23.89

[42] Kho, Yap Bing, Abid Hussanan, Norhafizah Mohd Sarif, Zulkhibri Ismail, and Mohd Zuki Salleh. "Thermal radiation effects on MHD with flow heat and mass transfer in Casson nanofluid over a stretching sheet." In *MATEC Web of Conferences*, vol. 150, p. 06036. EDP Sciences, 2018. https://doi.org/10.1051/matecconf/201815006036

[43] Raza, Jawad. "Thermal radiation and slip effects on magnetohydrodynamic (MHD) stagnation point flow of Casson fluid over a convective stretching sheet." *Propulsion and Power Research* 8, no. 2 (2019): 138-146. https://doi.org/10.1016/j.jppr.2019.01.004

[44] Sutton, George W., and Arthur Sherman. *Engineering magnetohydrodynamics*. McGraw-Hill, 1965.

[45] Abo-Eldahab, Emad M., and Mohamed A. El Aziz. "Hall and ion-slip effects on MHD free convective heat generating flow past a semi-infinite vertical flat plate." *Physica Scripta* 61, no. 3 (2000): 344. https://doi.org/10.1238/Physica.Regular.061a00344

[46] Buongiorno, Jacopo. "Convective transport in nanofluids." *ASME Journal of Heat and Mass Transfer* 128, no. 3 (2006): 240-250. https://doi.org/10.1115/1.2150834